

Sl. No.	<p style="text-align: center;">IIT Ropar List of Recent Publications with Abstract Coverage: July, 2025</p>
A	<p style="text-align: center;">Book(s)</p>
1.	<p><u>Immunotherapy in autoimmune disorders: Mechanisms and applications</u> <u>JN Agrewala - Book: ISBN: 9781003517023, CRC Press, 2026</u></p> <p>Abstract: This book offers a comprehensive review of the molecular and cellular mechanisms underlying autoimmune disorders, as well as the role of immunotherapy in managing these diseases. The initial chapter introduces the concept of tolerance, the immune system's capacity to distinguish between self and non-self. Further, it explores various factors that can disrupt this balance, leading to a breakdown of tolerance and the onset of autoimmune diseases. The book evaluates current strategies for managing autoimmune diseases, emphasizes their limitations, and introduces immunotherapeutic approaches. Furthermore, it delves into the latest advancements in immunosuppression, vaccine development, and the role of specific immune cells in autoimmune conditions. It discusses the generation of regulatory T cells (Tregs) and their therapeutic potential, as well as examines vaccines and myeloid-derived suppressor cells for preventing and treating autoimmune diseases. Additionally, the book addresses a revolutionary approach, chimeric antigen receptor T-cell (CART) therapy, for treating autoimmune disorders. Toward the end, the book examines the role of the gut microbiome on immune function and autoimmunity. It considers innovative drug delivery strategies as the future of personalized medicine in managing autoimmune diseases. This book is a valuable resource for researchers and students in immunology, microbiology, and pharmaceutical sciences. Key Features Explores promising new frontiers in next-generation immunotherapy for autoimmune diseases Reviews the role of factors leading to the loss of immune tolerance and existing autoimmune disease management Examines innovative drug delivery strategies and the therapeutic potential of nutraceuticals against autoimmune diseases Reviews the role and therapeutic potential of gut microbiome in autoimmune disorders Presents the therapeutic potential of Tregs, chimeric antigen receptor T-cell therapy, and myeloid-derived suppressor cells in treating autoimmune diseases</p>
B	<p style="text-align: center;">Book Chapter(s)</p>
2.	<p><u>Biomedical applications of biogenic carbon-based fluorescent nanoparticles</u> <u>K Kaur, G Singh, R Badru, N Kaur, N Singh - Biogenic Nanomaterial for Health and Environment: Book Chapter, 2025</u></p> <p>Abstract: The wide-ranging applications of carbon dots (CDs), which can be developed using either green or chemical precursors, have been made possible due to their reported properties and the various precursors that have been identified. This has opened up new opportunities for the development of high-quality CDs and their use in optoelectronic devices, bioimaging, and other applications. Green precursors can be derived from fruits, vegetables, flowers, leaves, seeds, stems, crop residues, fungi/bacteria species, and waste products, while chemical precursors can be categorized as either acid reagents or non-acid reagents. It provides a brief review of the past ten years of CD synthesis using both green and chemical precursors, as well as the use of CDs as sensing materials in biomedical applications. This comprehensive review will be a valuable resource for researchers who are interested in synthesizing high-quality CDs for a variety of applications.</p>
3.	<p><u>Building psychosocial resilience: A synthesis of previously conducted interventions</u> <u>P Singh - The Routledge International Handbook of Psychosocial Resilience: Book Chapter, 2025</u></p>

	<p>Abstract: Prevention of stress-related psychopathology has been a significant concern in the past, and resilience has always been the focus of related interventions. Resilience protects individuals from experiencing mental health problems despite being in a precarious state. Research findings indicate that resilience is malleable and can be enhanced through appropriately designed interventional programmes. Drawing on contemporary theories, researchers have developed diverse resilience training programmes, often implemented in face-to-face settings, both individually and in groups, tailored for various clinical and non-clinical populations. Despite a plethora of research on resilience interventions, a comprehensive understanding that can be practically applied to foster resilience in the youth is yet to be fully realised. The present chapter aims to contribute by synthesising the characteristics of interventions designed to foster resilience and mental health. It intends to offer insights for developing interventions for promoting resilience in individuals. In the first section, the chapter presents the conceptualisation of resilience and a brief overview of theoretical frameworks explaining resilience. Subsequently, it summarises the characteristics of the interventions devised to promote resilience, highlighting the identified protective mechanisms, possible ways to promote them, and some drawbacks observed. Finally, a summary of the current status of existing school-based interventions to foster resilience among individuals will be presented.</p>
4.	<p>Club convergence in growth and financial development: evidence from Indian States S Bardhan - 75 Years of Growth, Development and Productivity in India: Issues, Measures: Book Chapter, 2025</p> <p>Abstract: The paper revisits the issues of convergence in the context of economic growth across Indian states. Unlike existing body of literature on convergence in Indian context, we investigate the possibility of club convergence among Indian states. Using state level data of a sample of 33 states during 1985–2018, we first test whether Indian states converge in terms of per capita income. Subsequently, we examine, among few other channels of convergence of growth, the role of financial development across Indian states. Unlike most of the existing studies in India, we apply (Phillips & Sul, 2007) methodology to detect converging subgroups of states in terms of growth as well as various alternative indicators of financial development. Findings reveal that for the aggregate sample of states, there is no evidence of convergence, which implies that sample states are not converging to a single steady. However, we find evidence of the existence of club convergence. In particular, Indian states are found to diverge in terms of state level per capita growth as well as alternative indicators of financial development. Our empirical findings, however, reveal the formation of clubs in terms of both state level growth as well as various indicators of financial development such as branch density, different composition of sectoral credit and also indicators of credit inflow and credit outflow across states. Findings point to the prevalence of uneven growth and financial development across Indian states, despite several measures taken during the last few decades. Findings also call for concerted policy actions for achieving regional balance in growth and financial development through appropriate reform measures in investment, infrastructure and financial development.</p>
5.	<p>Slope stability analysis of rainfall-induced landslide, Malin, Maharashtra BK Yeshwantrao, N James - Intelligent Infrastructure and Smart Materials: Sustainable Technologies for a Greener Future: Book Chapter, 2025</p> <p>Abstract: This study examines the critical impact of continuous rainfall on the stability of the Malin slope, which experienced a catastrophic landslide in July 2014. To understand the relevant physics that initiated landslide, seepage and back analysis of the unsaturated slope were performed.</p>

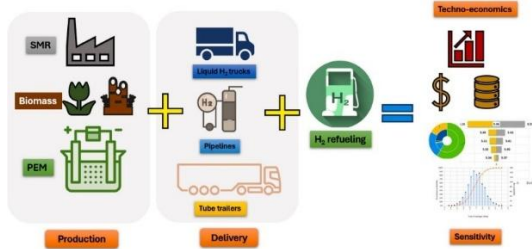
	<p>The results show that antecedent rainfall played a role in slope instability. Change in volumetric water content and pore water pressure also have a big impact on slope instability. The study provides a comprehensive analysis of the infiltration within the soil. The findings reveal significant moisture accumulation and rising pore pressures due to sustained rainfall, which progressively weakened the slope's stability. The Factor of Safety (FoS) decreased from 1.36 to 0.976, indicating failure. This research underscores the importance of integrating slope stability analysis with transient seepage monitoring to predict and mitigate rainfall-induced geotechnical hazards.</p>
C	<p style="text-align: center;">Conference Proceeding(s)</p>
6.	<p>A 2.9 mW inverter-based quadrature phase clock generator with $\pm 0.29^\circ$ phase error MK Singh, M Bhuvanesh, R Nagulapalli, DM Das, M Sakare - 2025 IEEE International Symposium on Circuits and Systems (ISCAS), 2025</p> <p>Abstract: The quadrature phase clocks are important elements in digital programmable transceivers in communication system applications. However, current solutions in quadrature clock generators for broad frequency ranges need more phase accuracy, and they suffer from substandard phase noise performance and excessive power consumption. To address these challenges, this paper proposes an inverter-based quadrature-phase clock (I-QPC) generator. The I-QPC generator utilizes inverters as delay elements to achieve the desired phase without using poly-phase type-1 filters because inverters are simpler to design and optimize for different phase delays. The system implements a phase-averaging mechanism using the delayed and interpolated signals, leading to quadrature-phase signals. The proposed technique has been validated in 28nm standard CMOS technology after post-layout parasitic extraction. The I-QPC generator operates over the broad frequency range (1GHz to 6GHz) and occupies an active area of 0.0005mm^2. The post-layout simulation results show that the phase error is $\pm 0.29^\circ$ while operating at 6GHz. The phase noise is -131.7dBc/Hz at an offset of 1MHz with a power consumption of 2.9mW. The I-QPC generator's figure of merit (FoM) is 217.3dBc/Hz at 1MHz offset frequency, which is better than state-of-the-art architectures. The performance of the I-QPC generator was further evaluated in hardware by implementing the circuit on a breadboard using the SN74HC04N inverter IC, and it demonstrated the successful generation of the quadrature signals at 1MHz frequency</p>
7.	<p>Air Sense: Internet of things-enabled novel power efficient indoor air quality monitoring system R Raina, KJ Singh, S Kumar - 2025 International Conference on Microwave, Optical, and Communication Engineering (ICMOCE), 2025</p> <p>Abstract: Air pollution, known to cause health issues such as respiratory and cardiovascular diseases emphasize the importance of monitoring indoor air quality with carbon dioxide (CO₂) sensor. Despite various air quality monitoring systems being discussed in the literature, their power consumption is often overlooked. This paper introduces Internet of Things (IoT) enabled novel power efficient indoor air quality monitoring system that uses CO₂, temperature and humidity sensors which send data to the cloud via Global System for Mobile Communication (GSM) technology. Moreover, keeping CO₂ levels below 1000 PPM is vital for optimal indoor air quality as discussed in literature. The CO₂ sensor operates continuously, while the temperature and humidity sensor activates when the CO₂ level becomes equal or exceeds 1000 PPM. By combining temperature and humidity data with CO₂ levels, a more thorough insight into air quality is achieved. This strategy will reduce the power consumption of the device as both the sensors are active when there is a critical need of monitoring. The system's battery life is approximately 9.71 days when CO₂ sensor is active only, decreasing to 8.71 days when both sensors are active using a 15600mAh/4.2 V battery. Furthermore, the sensor's fetching interval is set to 15 min when CO₂ values are unstable. However, when CO₂ values remain stable, the fetching interval starts at 15</p>

	min and doubles with each successive stage of continued stability. This approach minimizes the device's power consumption by reducing the frequency of data collection.
8.	<p>Anytime fairness guarantees in stochastic combinatorial mabs: A novel learning framework S Pokhriyal, S Jain, G Ghalme, V Aggarwal - Proceedings of the International Joint Conference on Autonomous Agents and Multiagent Systems (AAMAS), 2025</p> <p>Abstract: This paper proposes a novel framework for incorporating anytime fairness guarantees in a general Stochastic Combinatorial Multi-Armed Bandit (CMAB) problem when the time horizon is unknown. Our framework does not make any assumptions about the reward feedback or structure and provides fairness guarantees as long as a sublinear regret algorithm exists to solve the same problem. The framework essentially operates in the episodes of length H, which is a user-defined parameter. The framework divides each episode of length H into fairness rounds and learning rounds. Motivated by preemptive scheduling on uniform machines, we propose Fair-CMAB which prioritizes fairness rounds upfront and uses any existing CMAB algorithm for learning rounds. This helps in generalizing the framework significantly. Theoretically, we prove that for a sufficiently large value of H, Fair-CMAB achieves anytime fairness guarantees after some initial number of rounds and achieves the regret guarantees of the same order as the learning algorithm.</p>
9.	<p>Double integral sliding mode sensorless FOC for improved dynamics in IPMSM driven refrigerators AS Kiran, A Kumar, KR Sekhar, N Kumar - 2025 IEEE Industry Applications Society Annual Meeting (IAS), 2025</p> <p>Abstract: Considering the requirement of improved dynamics and noise-free operation in domestic refrigeration systems, this work proposes a double integral sliding mode vector control (DISMVC) strategy for the sensorless operation of interior permanent magnet synchronous motor (IPMSM). Addressing the peak overshoots due to the limited operational range in the conventional control strategies, the proposed DISMVC offers smooth control over the extended range of speed variations. The proposed double-integral sliding surface ensures instantaneous speed reference tracking and reduced peak overshoots. Further, to handle the chattering phenomena in conventional sliding mode control, a sigmoidal function is introduced instead of the traditional signum function in coherence with the double integral sliding mode control. The proposed control, along with the sigmoidal function, significantly reduces the current chattering and, thereby, torque ripple helps minimize the vibrational noise in refrigeration systems. The performance of the proposed sensorless IPMSM drive is validated through extensive MATLAB/Simulink simulations, followed by experimental testing on a refrigeration setup to demonstrate its effectiveness in real-world applications.</p>
10.	<p>Fairness driven slot allocation problem in billboard advertisement D Ali, S Banerjee, S Jain, Y Prasad - Pacific-Asia Conference on Knowledge Discovery and Data Mining, 2025</p> <p>Abstract: In billboard advertisement, a number of digital billboards are owned by an influence provider, and several commercial houses (which we call advertisers) approach the influence provider for a specific number of views of their advertisement content on a payment basis. Though the billboard slot allocation problem has been studied in the literature, this problem still needs to be addressed from a fairness point of view. In this paper, we introduce the Fair Billboard Slot Allocation Problem, where the objective is to allocate a given set of billboard slots among a group of advertisers based on their demands fairly and efficiently. As fairness criteria, we consider</p>

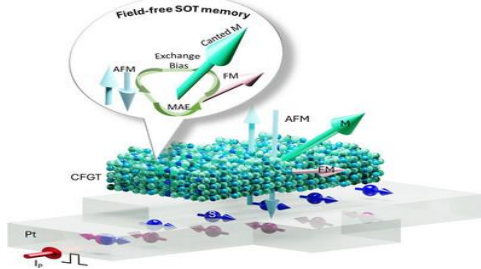
	<p>the maximin fair share, which ensures that each advertiser will receive a subset of slots that maximizes the minimum share for all the advertisers. We have proposed a solution approach that generates an allocation and provides an approximate maximum fair share. The proposed methodology has been analyzed to understand its time and space requirements and a performance guarantee. It has been implemented with real-world trajectory and billboard datasets, and the results have been reported. The results show that the proposed approach leads to a balanced allocation by satisfying the maximin fairness criteria. At the same time, it maximizes the utility of advertisers.</p>
11.	<p>Probable health risk of pollutants and noise found inside bottling beverage plant of Himachal Pradesh, India</p> <p>I Dhada, P Vats, B Singh - Indian International Conference on Air Quality Management, (IICAQM 2023), 2025</p> <p>Abstract: Rapid industrialization worldwide has led to a noteworthy rise in air pollution, affecting the indoor air quality of urban areas and posing health risks. This research precisely explored the impact of air pollutants and noise found within 12 bottling beverage industries dealing with alcohol, situated in Himachal Pradesh, India. The research focused on (TVOCs), noise, various sizes of particulate matter (PM_{2.5}, PM₁₀, PM₁), inhalable, thoracic, and alveolic PM, along with Black Carbon concentrations during the monsoon season. It also assessed the potential harmful impacts linked with these pollutants. The highest values of TVOC, PM₁₀, PM_{2.5}, PM₁, BC, and noise were found to be 142 ppm, 359 µg/m³, 102 µg/m³, 65 µg/m³, 26 µg/m³, and 87 dB, respectively. Non-carcinogenic health risk is found to be in the range of 4.7E-05–8.9E-05, and the age group 16–21 years males and females are more prone to non-carcinogenic risk. Carcinogenic risk due to BC is estimated to be in the range of 5.8E-04–6.8E-04, which is not significant. Due to ethical reasons and limited resources, the monitoring is restricted to one season, so the health actual risk will be less than the reported value here if annual average concentrations are considered.</p>
12.	<p>PV-battery integrated dual-CLLLC converter system for critical load applications with mode-adaptive power control</p> <p>S Saini, A Kumar, N Kumar, AS Kiran, A Patel, KR Sekhar - 2025 IEEE Industry Applications Society Annual Meeting (IAS), 2025</p> <p>Abstract: The increasing demand for reliable renewable energy solutions necessitates an effective power management, especially for critical load applications. This paper presents a PV-Battery Integrated Dual-CLLLC Converter System with an adaptive mode power control strategy to enhance energy efficiency and stability. The proposed dual-CLLLC resonant converter utilizes soft-switching to reduce losses, and improve performance of the system. A pulse frequency modulation (PFM)-based Maximum Power Point Tracking (MPPT) algorithm dynamically adjusts the switching frequency for fast and accurate MPP tracking under varying solar conditions. To ensure uninterrupted operation, a battery energy storage system (BESS) and an adaptive mode-selection algorithm enables smooth transitions between different power modes. Furthermore, the system's bidirectional power flow capability enhances energy exchange between the PV system, battery, and DC microgrid. The systems high efficiency, fast dynamic response, and improved reliability compared to conventional MPPT techniques are validated in the MATLAB Simulink software. This scalable and robust technique optimizes PV utilization, ensuring stable and uninterrupted power delivery for critical load applications.</p>
13.	<p>RRR: Rethinking randomized remapping for high performance secured NVM LLC</p> <p>PN Tanksale, GRS Seethiraju, S Das, VK Tavva - 2025 IEEE International Symposium on Hardware Oriented Security and Trust (HOST), 2025</p>

	<p>Abstract: As the workload footprint is increasing there is a need to increase the last level cache (LLC) size in processors. Increasing the LLC size with current SRAM technology is difficult because of stringent area and energy constraints. Non-volatile technologies like spin transfer torque RAM (STT-RAM) have been explored as an alternate to SRAM at LLC. However, STT-RAM comes with its own set of challenges of high write latency and energy. The community has seen a quantum of works that propose to mitigate the challenges of long write latency in STT-RAM LLC. On the other hand the community has also witnessed a stream of works pointing towards the cache contention based attacks at LLC and their countermeasures as well. This has lead to a chain of attacks and defence race at the LLC. Randomized caches at LLC is one such countermeasure gaining traction in the community. Ceaser, Ceaser-S, and Scatter-Cache are the state-of-the-art randomized caches. Going forward, integrating randomization with STT-RAM is crucial for enhancing both the security and performance of the STT-RAM LLC. In this paper, we observe, Ceaser, Ceaser-S, and ScatterCache exhibit a performance of -28.8%, -7.3%, and -6.5% respectively across a total of 97 SPEC CPU 2006, SPEC CPU 2017, and GAP workloads for a 4-core system in STT-RAM LLC compared to STT-RAM LLC with non-randomized cache. We then investigate the potential causes of the observed performance degradation and propose a technique, namely, Rethinking Randomized Remapping (RRR), which intelligently remaps cache blocks only in the Tag array of the LLC and strategically avoids accessing the Data array. Our approach significantly recovers much of the lost performance across various workloads. With RRR, the performance is around -11% for Ceaser, -3.9% for Ceaser-S, and -5.5% for Scatter-Cache for our workloads. Our experimental findings suggest that RRR conserves ~94% of dynamic energy per remapped block and reduces remap time by ~66% compared to traditional STT-RAM remapped caches.</p>
14.	<p>Towards enhanced reactive power margin for a Solar PV source through transformer interfaced dual VSC topology to support industrial grids M Kallamadi, A Kumar, AS Kiran, KR Sekhar - 2025 IEEE Industry Applications Society Annual Meeting (IAS), 2025</p> <p>Abstract: Reactive power requirements must be addressed in a timely manner by the utility to avoid the problems faced by vulnerable loads. At times, typical loads, such as nuclear reactors, will require momentary reactive power from the utility. In an attempt to replace conventional grids with renewable counterparts, the reactive power requirement is even more crucial. This work aims to support the utility grid with a solar photo-voltaic (PV) driven voltage source converter (VSC) under bulk reactive power requirements. Here, transformer-interfaced dual VSC topology (TIDVT) is used as an interfacing entity between the PV source and the utility grid. The control strategy for this system is explored to identify the supported features of the TIDVT topology. Eventually, better reactive power margins are being observed, which in turn will be beneficial to industrial grids feeding bulk reactive power consuming loads. The details of the control methodology used along with the experimental validation are explained.</p>
15.	<p>Valorization of biomass-based residue blended options for energy cogeneration SA Waziri, I Dhada, R Das - Recent Advances in Energy Transitions Towards Sustainable Development, (CHEMCON 2023), 2025</p> <p>Abstract: Synonymous with forestry activities and agriculture, waste generation has become a major issue of concern. Biomass has become an important sustainable and viable source of chemical energy capable of being converted into diverse energy manifestations whether through indirect or direct means. Globally, the integration of renewable options (biomass) into the energy stream continues to witness steady growth, catapulted by a range of factors which include minimal</p>

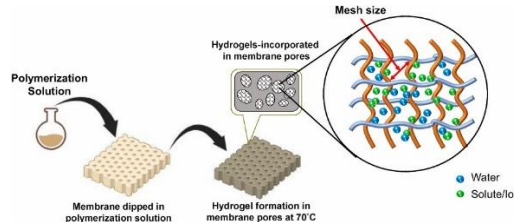
	<p>emissions, the quest for cleaner alternatives, heightened governmental provisions for renewable energy innovation, and the vast pool of unexplored prospects in biomass. In the context of Indian agriculture, which boast with a cropping intensity of over 140% and a cultivated area extending to 180 million hectares, a considerable volume of biomass is generated, with residues constituting a prominent share. In the Punjab region, biomass is readily available as agricultural waste throughout the year, which has been a persistent source of environmental pollution. This study aims to investigate the proximate and elemental composition of certain residues to evaluate their energy potential and blending suitability for heat and power generation. Poplar wood (<i>Populus ciliata</i>), eucalyptus wood (<i>Eucalyptus globulus</i>), sugarcane bagasse (<i>Graminae Saccharum officinarum</i>), coconut shell (<i>Cocos nucifera</i>), switchgrass (<i>Panicum virgatum</i>), and congress grass (<i>Parthenium hysterophorus</i>) were studied using thermochemical analysis; the ash content is $1.07 \pm 0\%$, $1.38 \pm 0.28\%$, $6.49 \pm 0.51\%$, $9.75 \pm 1.48\%$, $6.2 \pm 0.28\%$, and $9.7 \pm 0.42\%$ respectively. Volatile matter for poplar was $73.65 \pm 0.92\%$, eucalyptus was $74.3 \pm 1.84\%$, and their respective conceptual heating values (HHV) were 18.23 MJ/kg and 16.80 MJ/kg.</p>
D	Article(s)
16.	<p>A generalized modular battery pack topology with active cell balancing technique A Ahmad, AVR Teja, S Payami - IEEE Transactions on Industrial Electronics, 2025</p> <p>Abstract: This article presents a novel generalized modular battery pack with any “n” parallel battery strings of any “m” series connected cells where $((m, n) \in \mathbb{Z}^+)$. This novel battery pack prevents circulating current and also balances the entire battery pack using the proposed boost-based active cell balancing strategy. The proposed cell balancing topology employs only two active switches per cell and utilizes “n” inductors for a $m \times n$ cell battery pack, allowing efficient active balance throughout the pack. A detailed theoretical analysis is presented, and operating conditions are systematically derived to maximize output power and achieve optimal efficiency. The proposed topology and balancing technique are also simulated using MATLAB/Simulink for a three parallel strings of three series connected cells battery pack and the results are presented. These results are also experimentally verified using BAKH18650CIL battery cells in the laboratory. It could achieve cell balance while operating at 95.92% efficiency.</p>
17.	<p>A modified three stage dynamic comparator achieving rail-to-rail input common-mode range with < 86 fJ·ns EDP N Sharma, SA Thomas, V Hande, DM Das - IEEE Transactions on Circuits and Systems II: Express Briefs, 2025</p> <p>Abstract: This paper presents a high-speed, low kickback noise dynamic comparator featuring a modified three-stage architecture that demonstrates rail-to-rail input common-mode voltage ($V_{i,cm}$) operation. The proposed design utilizes parallel NMOS and PMOS pre-amplifier signal paths, which feed into a modified Strong-Arm latch. To ensure high-speed performance across the full 0-V_{dd} $V_{i,cm}$ range, a PMOS pre-amplifier and two-stage NMOS pre-amplifier are employed. The additional amplification stage between the NMOS pre-amplifier and the latch allows the use of NMOS input pairs in latch for NMOS pre-amplification stage as well. This architecture enhances $V_{i,cm}$ range and also improves kickback noise immunity by leveraging the complementary noise contributions of the NMOS and PMOS signal paths. The proposed comparator maintains $V_{i,cm}$ insensitivity and robust speed performance throughout the entire $V_{i,cm}$ range. Fabricated in 180-nm CMOS technology, the prototype achieves a relative CLK-Q delay of less than 210 ps and an energy-delay product (EDP) below 86 fJ·ns, for 1.8 V supply.</p>

18.	<p>A novel attack path detection framework considering cascading failures in an interdependent cyber–physical power system</p> <p>S Agarwal, R Sodhi - IEEE Transactions on Industrial Informatics, 2025</p> <p>Abstract: This article proposes a novel approach to identify the critical attack path (CAP), comprising of multiple cyber and physical components that an attacker may exploit sequentially, so as to cause maximum damage to the system. The proposed CAP detection framework (CAPDF) considers the jamming attack, which causes cascading failures on the individual cyber and physical layers. The framework involves three stages wherein, Stage-1 identifies the critical physical lines and cybernodes in the system. Due to the interdependence of the cyber and physical components, the cascaded effect of a critical component’s outage is evaluated in Stage-2. Finally, Stage-3 ranks the critical contingency sequence based on the multifactor decision analysis. Further, the proposed CAPDF is made robust against the stochastic nature prevailing in the system conditions, using a stochastic model and an ensembling mechanism. The proposed scheme is implemented using a MATLAB+NS3 co-simulation platform on the IEEE 14-bus system and the New England 39-bus system.</p>
19.	<p>A techno-economic evaluation of hydrogen production and delivery options for India's agricultural landscape</p> <p>S Sharma, AH Sahir - Sustainable Energy Technologies and Assessments, 2025</p> <p>Abstract: Hydrogen is a promising energy carrier amidst escalating concerns of environmental sustainability. This paper presents the first region-specific techno-economic analysis of hydrogen production pathways viz., steam methane reforming, biomass gasification, and polymer electrolyte membrane (PEM) electrolysis tailored to India’s agricultural landscape. Using US-DOE models (H2A, HDSAM, and HDRSAM), the analysis investigates H₂ delivery mechanisms through tube trailers, pipelines, and liquid hydrogen trucks. A case study focused on converting a Union territory’s bus fleet to hydrogen fuel cell electric vehicles is presented to examine end-use applications in the transport sector. Results show that the levelized cost of biomass gasification (\$8.77/kg with pipeline delivery) is comparable to conventional steam methane reforming (\$8.18/kg), suggesting a viable green alternative pathway leveraging agricultural residues. PEM electrolysis has the highest production cost (\$8.31/kg), increasing to \$14.31/kg with pipeline delivery. Delivery by liquid hydrogen is \$1–\$2/kg more expensive than gaseous pipelines. Risk analysis and Monte Carlo simulations highlight the breakdown of CAPEX and OPEX sensitivities as key cost drivers. The high CAPEX costs necessitate upfront financing, with a preferred debt-equity ratio of 60:40. Overall, this work provides strategic, data-driven insights for green hydrogen deployment in emerging economies, where agricultural resources and decentralized production might play a pivotal role.</p> 
20.	<p>Automatic diabetic retinopathy detection using an ensemble learning approach and classifiers with self-adjusting weights</p> <p>R Nadda, J Singh, U Shrivastava - Soft Computing, 2025</p>

	<p>Abstract: Diabetic retinopathy (DR), a common eye disease, can cause extreme damage to the vitals of the patients or even blindness. This disease can cause vision impairment and possibly full blindness in diabetic patients who do not receive the correct diagnosis and treatment in the early stages. Diabetic retinopathy must be detected early since the disease will gradually damage the eye. A computer-aided prognosis-based technique is currently being used to assist clinicians in identifying DR in its earliest stages. The existing approaches for classifying stages of DR have an inadequate ability to reliably detect early stages due to their inability to capture the complex underlying features. The present study aimed to automatically identify the stages of DR disease by evaluating retina image samples using a proposed ensemble machine learning approach with self-adjusting classifier weights. To improve the categorization of various stages of DR, the present study trained an ensemble of three deep Convolutional Neural Network (CNN) models and two machine learning models (ResNet50, Densenet121, Squeezenet1_0, SVM, and decision tree as base learners) using the openly accessible Kaggle dataset of retina pictures, to encode rich characteristics. The study results demonstrate that, in contrast to existing approaches, the proposed model identifies all stages of DR and outperforms state-of-the-art methods on the identical Kaggle dataset, with an accuracy of 98.35%.</p>
21.	<p>Biomass valorization with metal-free catalysts: innovations in thermocatalytic, photocatalytic, and electrocatalytic approaches A Chauhan, R Srivastava - Chemical Society Reviews, 2025</p> <p>Abstract: The catalytic valorization of biomass into high-value chemicals and sustainable fuels is critical for addressing global environmental challenges and advancing a bio-based circular economy. Traditional metal-based catalysts, though effective, face major limitations, including resource scarcity, toxicity, leaching, and cost, underscoring the need for alternative catalytic paradigms. Metal-free catalytic systems have emerged as promising sustainable solutions due to their environmental compatibility, cost-effectiveness, and material abundance. This review comprehensively evaluates recent progress in metal-free catalysis for biomass valorization, uniquely integrating and comparing thermal, photocatalytic, and electrocatalytic methodologies. We systematically discuss diverse classes of metal-free catalysts, including carbon-only materials, heteroatom-doped carbons, and emerging non-carbon frameworks, while highlighting advanced synthesis strategies, tailored active site engineering, mechanistic insights, and catalyst recyclability under varying operational conditions. The comparative analysis reveals distinct advantages and limitations inherent to each catalytic route, emphasizing the tunability and versatility of metal-free systems. Importantly, future proposed directions are rooted in the synergistic integration of photothermal and photoelectrochemical pathways, paving the way for next-generation multifunctional catalytic systems. By identifying persistent challenges such as active site localization, long-term stability, reaction selectivity, and scalability, the review advocates for interdisciplinary efforts incorporating advanced heterostructure design and AI-driven catalyst optimization to realize the full potential of metal-free catalysis in sustainable biomass valorization.</p> 
22.	<p>Boundary determination of coefficients appearing in a perturbed weighted p-Laplace equation N Kumar, T Sarkar, M Vashisth - Applicable Analysis, 2025</p>

	<p>Abstract: We study an inverse boundary value problem associated with p-Laplacian, which is further perturbed by a linear second-order term, defined on a bounded set Ω in $\mathbb{R}^n, n \geq 2$. We recover the coefficients at the boundary from the boundary measurements which are given by the Dirichlet to Neumann map. Our approach relies on the appropriate asymptotic expansion of the solution and it allows one to recover the coefficients pointwise. Furthermore, by considering the localized Dirichlet-to-Neumann map around a boundary point, we provide a procedure to reconstruct the normal derivative of the coefficients at that boundary point.</p>
23.	<p>Change point analysis in data with heavy tails: A normal inverse Gaussian approach M Rani, B Garg, A Kumar - <i>Economics Letters</i>, 2025</p> <p>Abstract: This article examines change points using the Normal Inverse Gaussian distribution that effectively captures heavy tails and skewness. We analyze the daily returns of fourteen major global stock indices from 2018 to 2024. Our methodology combines the Modified Information Criterion with Seeded Binary Segmentation and Greedy Selection. The analysis detects 7–17 change points per index, with primary clusters (5–12 indices) and secondary clusters (3–4 indices). Of note, the largest cluster emerges during the COVID-19 pandemic, underscoring methodology's effectiveness in identifying change points and the interconnectedness of global markets during crises. The findings also indicate increased market independence after the pandemic.</p>
24.	<p>Coexisting non-trivial Van der Waals magnetic orders enable field-free spin-orbit torque magnetization dynamics B Zhao, L Bainsla, S Ershadrad... - <i>Advanced Materials</i>, 2025</p> <p>Abstract: The discovery of van der Waals (vdW) magnetic materials exhibiting non-trivial and tunable magnetic interactions can lead to exotic magnetic states that are not readily attainable with conventional materials. Such vdW magnets can provide a unique platform for studying new magnetic phenomena and realizing magnetization dynamics for energy-efficient and non-volatile spintronic memory and computing technologies. Here, the coexistence of ferromagnetic and antiferromagnetic orders in vdW magnet $(\text{Co}_{0.5}\text{Fe}_{0.5})_{5-x}\text{GeTe}_2$ (CFGT) above room temperature, inducing an intrinsic exchange bias and canted perpendicular magnetism is discovered. Such non-trivial intrinsic magnetic order enables to realize energy-efficient, magnetic field-free, and deterministic spin-orbit torque (SOT) switching of CFGT in heterostructure with Pt. These experiments, in conjunction with density functional theory and Monte Carlo simulations, demonstrate the coexistence of non-trivial magnetic orders in CFGT, which enables field-free SOT magnetization dynamics in spintronic devices.</p> 
25.	<p>Composition-dependent pore structure and filtration performance of hydrogel-filled membranes V Sharma, SP Gumfekar - <i>Chemosphere</i>, 2025</p> <p>Abstract: Microfiltration (MF) membranes reject large-sized solutes ($>0.1 \mu\text{m}$) from feed streams. Filling up the MF pore space with porous polymers tailor solute rejection by virtue of membrane structure alterations. In this work, we synthesized poly(methacrylic acid-glycidyl methacrylate)</p>

(p(MAA-GMA)) hydrogels in polyethersulfone (PES) MF membrane pores and evaluated the role of hydrophobic GMA in membranes' structure, water transport, and performance under saline, oily, and real wastewater feed. Varying GMA concentration in hydrogel increased mesh size, thereby increasing membranes' permeability by 30 times compared to the p(MAA)-filled membrane. We quantified gel permeabilities using Happel's permeability model. Results indicated that hydrogels made from 0.05 M GMA contributed 22% to water transport, 15% more than p(MAA)-filled membrane. The membrane also showed hydrogel compaction effect during 24 h stability tests at 0.3 bar transmembrane pressure (TMP). Furthermore, we also found a drastic increase in permeate flux under CaCl_2 feed for GMA-containing membranes. All membranes showed salt retention at 5% permeate recovery, which formed the basis for estimating membranes' semi-permeability under each ion type using the Spiegler-Kedem-Katchalsky (SKK) model. When subjected to oily water feed, GMA containing membranes showed flux decline due to oil adsorption. However, none of the membranes did not show oil permeation. Textile wastewater filtration using PMG 5.0 showed COD reduction of 68% for high COD effluent, whereas, TDS reduced to 10% at 10% recovery with gradual flux increase under high-salinity effluent. Therefore, tailoring hydrogel compositions in MF membrane pores can potentially drive the applicability for industrial separations in upstream and downstream processes.

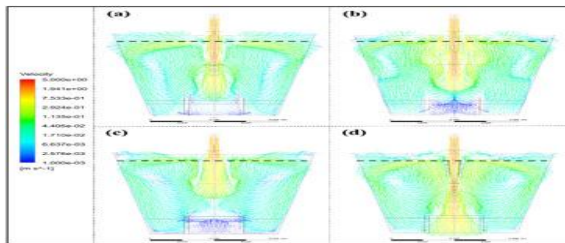


[Contribution of topographical and morphological parameters in glacier response to change in climate in the Western Himalaya](#)

S Guha, A Pratap, RK Tiwari, T Ghosh, D Gaikwad - Remote Sensing Applications: Society and Environment, 2025

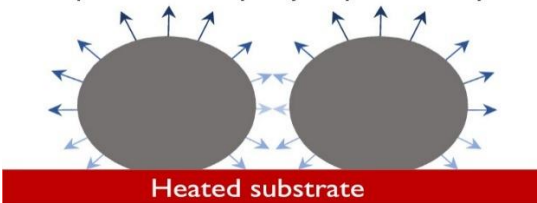
Abstract: Glacier thinning patterns are crucial in determining the availability and distribution of meltwater in Himalayan catchments, making precise assessments essential for predicting future water resources and formulating effective water management strategies. This study aims to quantify the specific influence of key topographic and morphological parameters on glacier thinning variability in the Himachal Himalaya and Kashmir Himalaya regions. Using Multiple Linear Regression, we systematically evaluate how maximum elevation, mean elevation, snout elevation, slope, aspect, glacier area, terminus type, and debris cover control variations in glacier thinning. To refine the model, a backward stepwise subset selection technique was employed to identify the most significant predictors, followed by least squares regression to quantify their contributions. The results reveal that in the Himachal Himalaya, glacier terminus type, mean elevation, and slope play dominant roles in influencing glacier thinning. Lake-terminating glaciers experience 0.23 ± 0.09 m/year more thinning than land-terminating glaciers, independent of other factors. Glaciers located 100 m higher in elevation exhibit 0.01 ± 0.004 m/year less thinning, while a 10 % increase in slope is associated with 0.19 ± 0.03 m/year less thinning. In the Kashmir Himalaya, debris cover extension, snout elevation, and glacier slope were identified as the primary controls on thinning heterogeneity. A 10 % increase in debris cover extension correlates with a 0.08 ± 0.02 m/year reduction in thinning, irrespective of other factors. Glaciers with snouts located 100 m higher in elevation experience 0.01 ± 0.003 m/year more thinning, even when controlling for debris cover and slope. Additionally, a 10 % increase in slope corresponds to 0.28 ± 0.04 m/year less thickness change compared to lower-sloped glaciers.

27.	<p>Convolutional and ℓ_{21}-norm neural network for bone age estimation MA Ganaie, J Rohan, K Agrawal, R Shah, A Girard, J Kasa-Vubu, M Tanveer - Applied Soft Computing, 2025</p> <p>Abstract: Bone age (BA) assessment is critical for evaluating children for potential endocrine, genetic and growth disorders. The evaluation of BA reading may vary among the readers. We use an Inception-v3 convolutional neural network to extract features and propose the novel ℓ_{21}-norm random vector functional link neural network (LR21-RVFL) for the automatic assessment of bone age. Random vector functional link neural network (RVFL) suffers in the presence of noise and outliers due to the squared loss function. To overcome these challenges, we incorporate an ℓ_{21}-norm-based loss function in the RVFL model to improve the robustness of the model. Moreover, we used ℓ_{21}-based regularization to suppress the redundant/irrelevant features and hence, generate a less complex model. The proposed LR21-RVFL model achieves better performance compared to baseline models (except R21-RVFL) in bone age prediction. Moreover, we evaluate the models on the classification of UCI and KEEL datasets.</p>
28.	<p>Development of adaptive moving window LSTM-EKF state and parameter estimator through maximum likelihood framework N Sabu, S Singh, J Valluru - The Canadian Journal of Chemical Engineering, 2025</p> <p>Abstract: For efficient control, monitoring, and online optimization of any processes, accurate information of the key process variables is critical. Data driven soft-sensors, which can predict the key quality variables using historical data, have gained significant attention in the process industry in the recent years. These soft-sensors are generally developed under normal operating conditions. In reality, chemical processes are subjected to abnormalities such as process parameter drift, sensor bias, or unmeasured disturbances. Under these abnormal conditions, the performance of data-driven soft sensors developed under normal data conditions will deteriorate over a period of time. To account for these data abnormality issues, soft-sensor models need to be adapted and robustified. In this work, a dynamic recurrent neural network-based state and parameter estimator is developed through moving window maximum likelihood framework. Initially, a machine learning state estimator is developed by integrating long short-term memory (LSTM) networks with the extended Kalman filter (EKF), which can estimate the critical quality variable using real-time process measurements. To address the data quality issues such as process drift and sensor bias, in the presence of measurement delays, an innovation error-based moving window maximum likelihood approach state and parameter estimator is proposed, where the LSTM integrated EKF is used as the state estimator. The performance of the proposed state and parameter estimator is evaluated on benchmark systems. From the analysis of results, it is observed that the proposed machine learning-based state and parameter estimator accurately estimates the states in presence of data abnormalities.</p>
29.	<p>Effect of backreaction on island, page curve and mutual information P Jain, S Pant, H Parihar - Nuclear Physics B, 2025</p>

	<p>Abstract: We compute the entanglement entropy of Hawking radiation in a bath attached to a deformed eternal AdS black hole. This black hole is dual to the two identical strongly coupled large-N_C thermal field theories, where each theory is backreacted (deformed) by the presence of a uniform static distribution of heavy fundamental quarks. In our observation we find that the entanglement entropy of Hawking radiation increases in a quadratic manner for an early time and linearly for the late time. The large time expression for the entanglement entropy of Hawking radiation is used to find the Page curve and Page time. After the Page time, the entanglement entropy saturates to a constant value due to the appearance of an island. We observe that introducing deformation (backreaction) delays the appearance of island and shifts the Page curve to a later time. Subsequently, the computation of the scrambling time reveals an increase with the backreaction parameter, suggesting a longer duration for information retrieval in the presence of deformation. Moreover, our analysis of the mutual information between the radiation subsystems shows that it vanishes at a critical time which increases with the deformation before the Page time. After the Page time, the appearance of island leads to the vanishing of mutual information between black hole subsystems and gives the time difference of the order of scrambling time.</p>
30.	<p>Effect of ladle shroud design on tundish hydrodynamic performance and attendant influence on tundish open eye A Maurya, PK Singh - Steel research international, 2025</p> <p>Abstract: Herein, three-phase numerical and experimental studies were performed to investigate the effect of various ladle shroud designs on the hydrodynamic performance of steelmaking tundish and size of the tundish open eye (TOE) formed. It is known that gas shrouding is necessary to prevent air ingress; however, it leads to the formation of TOE, which seriously impairs the steel cleanliness. This article considers a 0.35 reduced scale model of single-strand slab casting tundish fabricated using PERSPEX sheets, fitted with four different shrouds, namely, conventional ladle shroud (CLS), bell-shaped ladle shroud (BLS), reverse-tapered ladle shroud (RTL), and direct-tapered ladle shroud. The experimental and numerical investigations have been performed for gas-to-liquid loading ratios of 10%, 20%, and 30%. The numerical modeling has been done using volume of fluid method in ANSYS Fluent 2021R1 and is validated against the experimental results. With the use of BLS and RTL, significant improvement in tundish hydrodynamics can be observed when compared to CLS, as increase in plug flow varies from 10% to 25%, and decrease in dead region ranges from 15% to 35% at various gas-to-liquid loading ratios. Further, size of TOE decreases by $\approx 25\%$ with the implementation of BLS and RTL at higher gas-to-liquid loading ratio.</p> 
31.	<p>Effect of struts arrangements on lattice structures: Experimental and numerical approach Avinash, M Mursaleen, N Kumar - Mechanics of Solids, 2025</p> <p>Abstract: Lattice structures are employed in the aerospace, automotive, and medical industries due to their high energy absorption, high porosity, and high strength-to-density ratios. Besides the traditional manufacturing approach, here we employed additive manufacturing, Fused deposition modeling (FDM) approach. In this paper, effect of struts on compressive deformation behavior of Body-centered cubic (BCC), Helix body-centered cubic (HBCC), Half vertical strut body-centered</p>

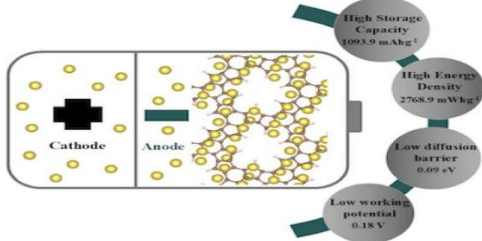
	<p>cubic (HVSBC) and Full vertical strut body center cubic (FVSBC) structures are examined both numerically and experimentally. The results show that the half verticle strut body center cubic has superior properties. The compressive strength of the Half vertical strut body-centered cubic (9.5 MPa) is ~436.72% higher than simple body-centered cubic (1.77 MPa), ~139.89% higher than the helix body-centered cubic (3.96 MPa), and ~25% higher than full vertical strut body-centered cubic (7.6 MPa). Also, the energy absorption of half vertical strut body-centered (3.49 MJ/m³) is ~14817.39% higher than the simple body-centered cubic (0.23 MJ/m³), ~711.62% higher than the helix simple cubic (0.43MJ/m³) and ~36.8% higher than the full vertical strut body-centered cubic. Further, the strut variation among structures controls the Poisson ratio and ultimately the strain-induced deformation response. Hence, optimizing local strut alignments in the lattice structures guides to betterment of mechanical properties for varied applications.</p>
32.	<p>Enhancing performance in worst-case scenarios of ble periodic advertising for dense IoT networks LK Baghel, G Shan - IEEE Internet of Things Journal, 2025</p> <p>Abstract: In dense Internet of Things (IoT) networks, where numerous devices transmit simultaneously, the conventional periodic advertising scheme, with its fixed advertising period, results in persistent collisions, leading to significant delays and higher energy consumption. These issues become more pronounced as the network grows. To overcome these limitations, this work proposes a novel adaptive periodic advertising scheme that dynamically adjusts the advertising period for each device for each transmission, effectively reducing collisions, improving delay performance, and enhancing energy efficiency. Based on the proposed scheme, an analytical framework is developed to analyze delay and energy consumption. In addition, an analytical expression determining the schedule of each advertiser, perfectly syncing the scanner for efficient reception, is derived. As a result, it significantly improves the reliability of the proposed scheme. Furthermore, based on analytical framework, simplified closed-form expressions are derived to choose the optimal advertising period. Moreover, based on these closed-form analytical expressions, algorithms are proposed that autonomously optimize the delay in such applications. The performance of the proposed scheme has also been compared with conventional periodic advertising scheme, and it is found that the proposed scheme outperforms conventional scheme in terms of delay and energy. Lastly, analytical results were validated using a custom-built simulation framework based on the widely recognized Riverbed Modeler (formerly OPNET).</p>
33.	<p>Evaluating crop yield prediction models in illinois using aquacrop, semi-physical model and artificial neural networks V Gautam, A Gani, S Pathak, AK Shukla - Scientific Reports, 2025</p> <p>Abstract: Crop yield is important for agricultural productivity and the country's economy. While crop yield estimation is an essential aspect of modern agriculture, it continues to be one of the most challenging tasks to manage effectively. Corn and soybean are the important crops in Illinois, USA, considerably enhancing the region's agricultural output and economy. The present study integrates semi-physical model, AquaCrop and Artificial Neural Network (ANN) Models for estimating corn and soybean yields. Data of different meteorological parameters including precipitation, maximum and minimum temperature, relative humidity, wind speed, solar radiation, photosynthetically active radiation and fraction of photosynthetically active radiation, land surface water index were collected for a period of 25 years from 2000 to 2024 from NASA POWER, USDA and NASS. The observed yield of soybean and corn was ranges from 2.49 to 4.37 ton/ha and 7.06 to 14.66 ton/ha. The predicted corn yield using the AquaCrop, semi-physical, and ANN models ranged from 7.60 to 14.42 ton/ha, 9.01 to 13.42 ton/ha, and 6.81 to 15.63 ton/ha, respectively. For soybean, the predicted yield ranged from 2.80 to 4.34 ton/ha, 2.92 to 3.84 ton/ha, and 2.45 to 4.43 ton/ha, respectively. The ANN model achieves the highest coefficient of</p>

	<p>determination ($R^2 = 0.96$) in predicting soybean yield, while the semi-physical model records the lowest R^2 value of 0.42, indicating the superior predictive capability of the ANN model. For both corn and soybean yields, the ANN model showed the highest prediction accuracy among the other models. Thus, the study underscores the significance of employing the ANN model for crop yield estimation, particularly in the regions that share similar physiographic and meteorological conditions with Illinois.</p>
34.	<p>Evaluation of undrained breakout capacity of shallowly buried plate anchors in cohesive soils using a tension-truncated Tresca strength criterion R Ganesh - Ocean Engineering, 2025</p> <p>Abstract: Plate anchors are widely used to provide economical mooring systems for many offshore infrastructures. Previous studies examining the undrained breakout capacity of plate anchors in purely cohesive soils were predominantly based on the classical Tresca (CT) strength criterion, which assumes equal uniaxial yield strengths in compression and tension. However, the observed uniaxial tensile strength of cohesive soils is often much lower than its compression counterpart, emphasizing the need to consider realistic tensile strength in practical engineering applications. This research investigates the potential impact of a tensile strength cutoff on the ultimate undrained breakout capacity of shallowly buried horizontal plate anchors in purely cohesive soils, utilizing a tension-truncated Tresca (TT) strength criterion. The analysis employs the discrete sum method based on horizontal slices within the upper bound plasticity theory to calculate the undrained breakout capacity of plate anchors under varying shapes, including circular, square, rectangular, and strip. A comparison of results obtained using both CT and TT strength criteria reveals a significant effect of the tension cutoff on the ultimate undrained breakout capacity of plate anchors in cohesive soils. Additionally, the study explores the influence of different anchor-soil interface conditions and the associated breakout failure surfaces under typical parameter combinations. Remarkably, the results of this study align well with the available numerical and experimental results in the existing literature.</p>
35.	<p>Evaporation of sessile drops on a heated superhydrophobic substrate S Kavuri, CS Sharma, G Karapetsas, KC Sahu - Langmuir, 2025</p> <p>Abstract: We experimentally investigate the evaporation dynamics of sessile water droplets on a micronano textured superhydrophobic aluminum substrate at various temperatures using shadowgraphy imaging. By comparing the evaporation behavior of two droplets placed side-by-side with that of an isolated droplet, we find that droplets in the two-drop system evaporate more slowly due to the vapor shielding effect, which increases vapor concentration between the droplets. This leads to asymmetric evaporation and longer lifetimes, particularly at room temperature compared to higher temperatures. At room temperature, the isolated droplet primarily follows a constant contact angle (CCA) mode, with occasional stick-slip events. The two-drop system predominantly exhibits CCA mode for most of its lifetime, with mixed-mode evaporation and some stick-slip behavior. At elevated temperatures, the isolated droplet maintains a nearly constant contact angle for the first half of its lifetime, transitioning to a mixed evaporation mode with occasional stick-slip events. In contrast, the two-drop system follows a mixed evaporation mode throughout, with occasional stick-slip behavior. Furthermore, a comprehensive theoretical model that accounts for diffusion, evaporative cooling, and convection accurately captures the evaporation dynamics of sessile droplets on a superhydrophobic substrate in both isolated and paired configurations at elevated substrate temperatures. In contrast, a diffusion-based model alone adequately describes the evaporation behavior at room temperature.</p>

	<p style="text-align: center;">Evaporation of Superhydrophobic Drops</p>  <p style="text-align: center;">Heated substrate</p>
36.	<p>Expected health risk out of black carbon and particulate matter in the indoor environment of an industrial cluster of Chandigarh in India I Dhada, SA Waziri, Vishal, S Singha, BK Padhi, SK Samal - Scientific Reports, 2025</p> <p>Abstract: The global increase in industrialization and its attendant exponential air pollution has posed a significant hazard to the indoor pollution levels of cities and the associated health risks. This study evaluated the health effects of air pollutants discovered inside the bottling industries in Chandigarh cluster in India. PM₁₀, PM_{2.5}, PM₁, and black carbon concentrations in the post-monsoon season were monitored, and associated health implications and lung disease were estimated. A positive correlation is established between PM in indoor and outdoor environments. Maximum concentrations for PM₁₀, PM_{2.5}, and PM₁ were recorded as 276.8 µg/m³, 97.7 µg/m³ and 66.5 µg/m³ (for indoor) respectively, which are approximately 15 and 6 times higher than their (PM₁₀ and PM_{2.5}) allowable concentrations set by World Health Organization, posing a health threat to the workers and staff of the industries. The lifetime carcinogenic risk of black carbon and the non-carcinogenic risk of particulate matter and black carbon have been assessed using a deterministic and probabilistic model, which shows the marginal difference. The estimated lifetime carcinogenic risk due to black carbon for males and females was observed in the range of 7.20E-05 to 6.17E-05. The spirometry analysis indicates that about 13.04% of the sample population (out of 184 samples) have healthy lungs.</p>
37.	<p>Explicit analytical model of stretchable interconnects for flexible electronics system G Bhatti, Y Agrawal, V Palaparthi, MG Kumar, R Sharma - IEEE Transactions on Signal and Power Integrity, 2025</p> <p>Abstract: A printed circuit board (PCB) is one of the strong backbones to execute electronic system designs. Due to fast and reliable communication requirements between integrated circuit and other peripheral components over the PCB, there is a quest for the development of board-level designs and layouts. The advancement in technology has led to inventions from conventional rigid to flexible PCBs or flexible electronics (FE). The conformability of FE circuitry majorly depends upon the stretchable interconnects. An interconnect is the medium through which a signal is transmitted. The characteristic of stretchable interconnects is determined through their electrical and mechanical properties. The analytical model and parasitic extraction of the interconnect for rigid PCB structures have been widely explored earlier. However, the analytical formulation of the stretchable interconnect still remains a challenge and meagerly explored till date. Consequently, in this work, an explicit analytical model for the parasitic extraction of stretchable interconnects, viz., resistance (R), inductance (L), and capacitance (C), under stretching and bending effects has been novelly proposed. Five different interconnect materials have been considered for the analysis. The analytical model results have been validated with the ANSYS EDA tool. It is investigated that the proposed analytical model results are in very close agreement with the ANSYS results for all the considered cases.</p>
38.	<p>Experimental and numerical investigation on compressive behavior of polymeric cell foam structures Avinash, M Mursaleen, N Kumar - Journal of The Institution of Engineers (India): Series C, 2025</p>

	<p>Abstract: Cellular structures are widely used in compressive applications as an energy absorbing and impact shield materials. The compressive behavior of polymer foam structures, having different pore sizes 3 mm, 3.5 mm, and 4 mm is evaluated experimentally and numerically. Fused deposition modeling process was employed to manufacture the structures. The effect of pore size on the compression behavior of the polymeric sample was evaluated under low quasi-static loading rate. The results present the energy absorption capacity of the foam structure having (pore dia.= 4 mm) is higher than others. The energy absorption of structure (pore dia.=4 mm) (2.4 MJ/m^3) is $\sim 990.9\%$ higher than solid (0.22 MJ/m^3) having the same size, and 152.6% higher than structure having 3 mm pore diameter (0.95), and 50.9% higher than 3.5 mm pore diameter (1.59 MJ/m^3) structure. The specific energy of foam (pore dia. = 4 mm) is also higher than others. The study reflects the effect of porosity to design foams structures for various energy absorbing applications.</p>
39.	<p>Extended depth-of-focus femtosecond laser pulses for flexible micromachining AN Jena, TM Hayward, A Kumari... V Pal - Optics Letters, 2025</p> <p>Abstract: We present a simple and efficient method for extending depth-of-focus of intense femtosecond (fs) pulses with a flat and thin multilevel diffractive lens (MDL). The MDL focuses fs-pulses at a desired distance, which remains invariant over an extended range of propagation distances, several times beyond that of a traditional lens. We have presented the results of strongly focused fs-pulses with different extended depth-of-focus obtained by two different MDLs. Further, we have shown laser filamentation with long plasma channels. We have also performed laser marking/machining in glass material with approximately constant spatial resolution over an EDOF. These findings can be exploited for high-throughput compact in-line fs-micromachining, potentially useful in micro-optics, microfluidics, and nanosurgery.</p>
40.	<p>FDI spillovers, innovation and the role of industrial clusters: evidence from innovative indian manufacturing firms P Chetia, SR Behera, T Mishra, M Parhi - Economic Modelling, 2025</p> <p>Abstract: This paper studies the impacts of horizontal and vertical foreign direct investment (FDI) spillovers on innovation activities of Indian manufacturing firms by comparing effects within major industrial clusters with those outside. We find that a great breadth of innovations arises via horizontal linkages among firms within the industrial clusters. Conversely, firms outside industrial clusters do not portend measurable innovation effects from FDI spillovers. Our results highlight the crucial role of geographical proximity in harnessing innovation spillovers, further emphasizing the need for tailored policies for firms outside major industrial clusters to maximize their innovation potential. A Difference-in-Differences estimation to gauge the effect of the 2014 FDI liberalization policy on firms' innovation output shows that foreign firms have significantly increased their innovation activities relative to domestic firms post-2014 FDI liberalization policy.</p>
41.	<p>Finite blocklength analysis of active RIS-assisted DDTW communication with hardware impairments S Kumar, B Kumbhani, G Kaddoum - IEEE Wireless Communications Letters, 2025</p>

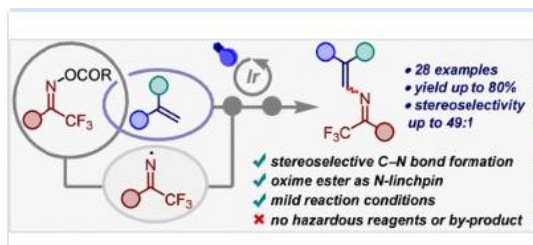
	<p>Abstract: This letter investigates the performance of active reconfigurable intelligent surface-assisted full-duplex-two-way communication in the presence of hardware impairments over Rician fading channels under the finite blocklength regime. We derive novel analytical expressions for average block error rate (ABLER) and ergodic capacity (EC). Additionally, system throughput, goodput and latency are also discussed. Asymptotic analysis for ABLER and EC is also done to gain useful insights. Monte Carlo simulations were performed to verify the analytical results. Numerical results revealed the superior performance of the active reconfigurable intelligent surface-assisted full-duplex-two-way system as compared to its passive counterpart and conventional full-duplex-two-way amplify and forward (AF) and full-duplex-two-way decode and forward (DF) relay systems. Index Terms—Active reconfigurable intelligent surface, finite blocklength, full-duplex, and loop interference.</p>
42.	<p>Functional boronic acid materials for cell surface interaction: Emerging applications in imaging and cellular transportation BK Das, J Gao, A Bandyopadhyay - Coordination Chemistry Reviews, 2025</p> <p>Abstract: The interplay between sp^2 and sp^3 hybridization at physiological pH empowers boron as a ‘magic element’ in numerous biomedical applications. The dynamic nature of boronic acid (BA)-mediated bioconjugation stands out as the most attractive feature, which enables a diverse range of claims. Among them, BA-mediated cellular imaging and cell entry stand out as versatile and promising strategies in the literature. This article systematically reviews the emerging applications of BA in imaging and cellular delivery. From the chemistry and materials perspective, we delineate the design principle of BA derivatives and their mechanism of cell surface interactions. In detail, the account of the article emphasizes the borono-lectins, –peptides, –transporters, –polymers, –liposomes, –proteins, –nanomaterials, and so on, which will attract a wide range of engaging readers. Ultimately, the review provides insights into BA's importance and perspectives for designing novel entities for future diagnosis and therapeutic applications. We believe this article will guide and encourage new-generation scientists to develop novel dynamic materials for multidirectional applications.</p>
43.	<p>Hierarchical motion magnification J Singh, SK Vipparthi, S Murala, GSR Kosuru... - Neurocomputing, 2025</p> <p>Abstract: Video motion magnification amplifies small, imperceptible variations, making them perceptible. It has a wide range of applications, such as measuring respiratory signals, classifying micro-expressions, measuring micro-displacements from a distance etc. Moreover, its applications are continuously expanding. Existing handcrafted techniques provide less effective solutions, often delivering lower magnification and requiring the selection of complex hyper-parameter values that vary across videos. To tackle these issues, deep-learning-based approaches are being introduced. However, they are sensitive to noise-related distortions during motion magnification. In response to these challenges, we propose a more robust hierarchical network for video motion magnification. To mitigate distortions that may arise from the magnification of noise and other illumination changes, we introduce a multi-scale manipulator with an edge-based input before magnification. Additionally, we propose a novel contrastive learning-based loss to further enhance the robustness of the magnification process against noise. To improve texture quality, we introduce a multi-resolution magnification generation architecture with a magnification decoder block. It produces hierarchical magnification from lower resolution to higher resolution. We compare the results of the proposed network both qualitatively and quantitatively with the state-of-the-art methods on synthetic and natural videos. Also, we conduct an ablation study to analyze various</p>

	modules of our method. The results demonstrate that our proposed base and lightweight models outperform the current state-of-the-art methods.
44.	<p>Holey penta-hexagonal graphene as an anode in high-efficiency sodium-ion batteries M Kaur, TJ Dhilip Kumar - ACS Applied Energy Materials, 2025</p> <p>Abstract: In this study, we inspect the suitability of the holey penta-hexagonal graphene (HPhG) nanolayer as an encouraging negative electrode material for sodium-ion batteries (SIBs), utilizing the density functional theory as the computational framework. Our structural analysis confirms that the HPhG system exhibits both thermal and dynamic stability. Electronic property investigations reveal that the pristine HPhG monolayer behaves as a semiconductor with a bandwidth of 0.28 eV. Remarkably, following the loading of one Na atom, the electronic nature undergoes a transformation from semiconducting to metallic, enhancing its conductivity. The HPhG monolayer demonstrates a substantial sodium storage capacity, with a theoretical value of 1093.91 mAhg⁻¹ and an associated energy density of 2768.91 mWhg⁻¹. Additionally, the material shows an excellent ion mobility, indicated by a small diffusion barrier of 0.09 eV and an elevated migration coefficient of $1.1 \times 10^{-3} \text{ cm}^2 \text{ s}^{-1}$, facilitating rapid charge–discharge cycles. The computed open-circuit voltage of 0.18 V is also within the optimal range for secure and sustainable battery operation. Additionally, the HPhG nanolayer in the SIBs exhibits adequate wettability toward various solvent molecules. These results collectively underscore the potential of the HPhG nanolayer as an advanced anode material for next-generation SIBs.</p> 
45.	<p>Impact of carbon sequestration technologies on corrosion resistance of various concrete types SK Saikia, AS Rajput - Construction and Building Materials, 2025</p> <p>Abstract: Concrete mineralization has recently received significant attention owing to its ability to enhance strength through microstructural densification apart from capturing atmospheric CO₂ (a greenhouse gas). This study attempted to understand the durability effects of sequestration performed during mixing and curing stages on conventional as well as green binder-added concrete types utilizing state-of-the-art mixing and curing setups. The conventional concrete was prepared using 100 % ordinary portland cement (OPC) as the binder. On the other hand, for developing the green concrete types, 50 % replacement of OPC was done separately with ground granulated blast furnace slag (GGBFS) and electric arc furnace (EAF) ash, respectively, along with using an alkali-activator. Various tests were performed to evaluate the performance of the developed concrete's strength, CO₂ uptake, porosity, and durability (such as charge passage, chloride penetration, chloride migration, and corrosion). It was observed that upon sequestration, CO₂ uptake capacity could be improved up to 25.17 % for OPC concrete, 19.96 % for GGBFS-added concrete, and 17.63 % for EAF ash-added concrete. In addition, the chloride penetration depth was reduced to 10.56 mm in the sequestered specimens, with a lower migration coefficient and charge passage of $2.36 \times 10^{-12} \text{ m}^2/\text{s}$ and 1510 C, respectively. Further, the experimental mass losses in rebars of reinforced concrete specimens during accelerated corrosion were lesser than the theoretically predicted values by up to 60 % in the sequestered ones.</p>

46.	<p>Influence of radio frequency magnetron sputtering on the microstructure, mechanical Properties, and wear performance of NiTi alloy coating on bearing steel</p> <p>T Ashraf, PK Vangara, T Narayana, DK Naik, S Saleem, KV Gopal - <i>Journal of Materials Engineering and Performance</i>, 2025</p> <p>Abstract: NiTi thin coatings are increasingly explored to enhance the performance of bearing steel (AISI 52100) components in engineering applications due to their superior mechanical and tribological properties. In this research, NiTi thin coatings were deposited on bearing steel substrates using radio frequency magnetron sputtering. The deposition process was conducted with power densities of 1.72 W/cm² for Ni and 2.96 W/cm² for Ti, at a working pressure of 0.4 Pa. The microstructure, mechanical, and tribological properties of the coating were characterized using a range of techniques, including GI-XRD, FESEM, EDS, nanoindentation, scratch testing, 3D surface analysis, and ball-on-disk tribological testing. The composite interlayer developed columnar dendrites extending toward the NiTi coating layer, with a gradient distribution of Ni and Ti elements observed in the elemental spectra. The NiTi coating demonstrated a hardness of 7.57 GPa, marking a 33.9% improvement compared to the AISI 52100 substrate. The tribological performance of the coating was evaluated against a Si₃N₄ ball using a reciprocating ball-on-disk tribometer under varying loads. The NiTi-coated specimens exhibited superior wear resistance compared to the uncoated AISI 52100 substrate under identical conditions. The NiTi coating achieved the lowest coefficient of friction (0.036) at a 1.5 N sliding load and the minimum wear rate (3.39×10^{-6} mm³/N m) at a 1.25 N sliding load.</p>
47.	<p>Influence of two-color pump and laser chirp on resonant harmonic generation in MoS₂ nanoflakes doped with Ni quantum dots and carbon nanotubes</p> <p>M Venkatesh, VV Kim, GS Boltaev, SR Konda, A Srivastava, TP Yadav, J Yu, P Svedlindh - <i>Optical and Quantum Electronics</i>, 2025</p> <p>Abstract: Wavelength-tunable coherent extreme ultraviolet sources generated via high-order harmonic generation (HHG) offer a range of unique and diverse applications. Here, we demonstrate the generation of intense, tunable, high-order harmonics from the laser-induced plasmas of molybdenum disulfide (MoS₂) materials containing Ni quantum dots and Ni-carbon nanotubes. We systematically explored the spectral characteristics of high-order harmonics by exciting with a two-color pump and varying the pulse duration and delay between driving and heating pulses. The two-color pump and laser chirp variations during HHG studies allow for achieving intense resonant 26th harmonic (30.7 nm) and tunable resonant-enhanced harmonics in the range of 31–37 nm, respectively. We show that the harmonic yield and cutoff from the MoS₂ plasma produced by picosecond heating pulses are higher compared to those from the plasmas produced by nanosecond pulses.</p>
48.	<p>Investigating in-structure acceleration amplification factor of RC frames using explainable artificial intelligence</p> <p>I Latif, M Surana, A Banerjee - <i>Structures</i>, 2025</p>

	<p>Abstract: The in-structure acceleration amplification factor (IAAF) plays an important role in designing the connections of secondary systems with the buildings. The methodology to obtain this factor is computationally complex and inadequately understood due to its dependence on material, ground motion, and structural characteristics. Here, we address this challenge by proposing a novel machine learning (ML) based methodology to predict the IAAF and explainable artificial intelligence to understand its dependence on the input parameters. We generated 50 unique sets of material properties through Latin hypercube sampling, corresponding to each of 4-, 8-, and 12-storey reinforced-concrete buildings to create a diverse dataset. The developed set of buildings was analyzed using a suite of 30 pulse-type ground motions to obtain the IAAF at different levels of inelasticity (ductility demands) in the buildings. The ML models trained on this diverse dataset to predict the IAAF achieved R^2, RMSE, and MAE of 0.96, 0.19, and 0.11, respectively, on the unseen test set. The model predictions were interpreted through a game theory-based approach of SHAP analysis, which revealed that structural and ground motion characteristics exhibited greater influence on the IAAF than material characteristics. It was also identified that the three most influential structural characteristics were relative floor level, strength ratio, and fundamental period of the building. Further, the influential ground motion characteristics comprise peak ground acceleration, peak ground velocity, and pulse period. The unconfined compressive strain and strength of concrete and the yield strength of steel are the three most important material parameters governing the IAAF predictions. Finally, an interactive dashboard was developed that allows users to obtain the predictions using the trained model and compare it with the values obtained using major building codes (ASCE 7–22, EC8, and IS 16700).</p>
49.	<p>IoT-Enabled energy-efficient and long-range solution for remote patient monitoring using Bluetooth low energy 5. x</p> <p>R Verma, S Gautam, NS Bal, S Kumar, N Saeed - IEEE Journal of Radio Frequency Identification, 2025</p> <p>Abstract: The Internet of Things (IoT) has revolutionized Remote Patient Monitoring (RPM) by enabling real-time data transfer. Traditional systems suffer from high energy usage and limited range, making them less suitable for long-term monitoring. This paper presents a novel wearable sensor node leveraging latest Bluetooth Low Energy (BLE) 5.0 features, such as long-range communication and energy-efficient extended advertising. The system integrates an ultra-low-power ARM M33 MCU, a motion sensor for activity tracking, and cloud connectivity for remote monitoring. The Physical Layer (PHY) modes, which determine on-air data transfer, significantly impact communication reliability. Challenges like packet loss are common, especially at extended ranges. Typical solutions involve increasing transmit power or implementing retransmission strategies, each with energy implications. The proposed system pioneers the evaluation of BLE modes—LE 1M and LE Coded PHY—on energy consumption and data transfer reliability of a broadcaster for sensor data transmission in real-time clinical settings. Experimental results reveal that while the conventional LE 1M reduces data transfer time by 84.92%, it increases Packet Loss Rates (PLR). In contrast, the latest LE Coded PHY reduces packet loss to just 2% at ranges upto 300 m but decreases battery life by 42.58%, still allowing a projected 2.6-year lifespan. To address power consumption, we propose a Dynamic PHY Switching Algorithm (DPSA) that adapts PHY modes. Results are validated on an IoT platform, providing insights for selecting BLE PHY for energy-efficient e-healthcare beacons.</p>
50.	<p>Ir (III)-Photocatalyzed stereoselective synthesis of 2-azadienes</p> <p>B Paul, S Samanta, S Das, I Chatterjee - Organic Letters, 2025</p>

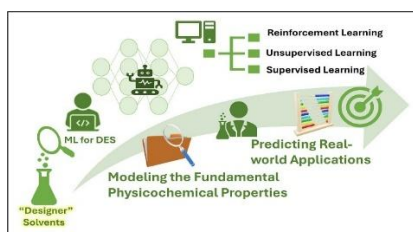
Abstract: A photocatalyzed, stereoselective C–N bond formation reaction was developed to synthesize 2-azadiene scaffolds containing trifluoromethyl groups under mild reaction conditions. This current methodology employs the multitasking photocatalysis of *fac*-Ir(ppy)₃ to generate iminyl radicals from bench-stable oxime-ester precursors via an energy transfer (EnT) mechanism. This iminyl radical is installed in the olefinic system as an *N*-linchpin without any prefunctionalization through a photoredox cycle. The advantages of the reaction consist of mild aerobic reaction conditions, broad scopes, high yield, and impressive stereoselectivity.



[Machine learning-driven optimization of Deep Eutectic Solvents: Accelerating physicochemical properties modeling](#)

S Saini, A Sharma, N Saini, N Kaur, N Singh - Sustainable Materials and Technologies, 2025

Abstract: Machine learning (ML) algorithms have made the analysis of vast datasets faster, thus revolutionizing the identification of multiplex correlations, composition optimization, along with accurate prediction of desirable properties. An exact assessment of key physicochemical properties must happen for optimizing Deep Eutectic Solvents (DES) applications. If we talk specifically, in uncovering precise molecular properties through advanced machine learning approaches, such as Random Forests (RF), Support Vector Machines (SVM), and Artificial Neural Networks (ANN) have been employed. Through rational design, the combination of ML with Deep Eutectic Solvents (DES) validates a new method for sustainable green solvents. Now, we can see through predictive modeling that solvent development excels by implementing data-based decisions that require much fewer resources and minimize market time while maintaining sustainability benchmarks. And besides potential opportunities for utilizing artificial intelligence to speed up DES improvement, we moreover look at the challenges, such as those related to data scarcity, model interpretability, and experimental approval. To sum up, this review delivers a clear understanding of how ML approaches DES property modeling by exploring myriad ML techniques together with feature selection methods, data limitations, and modeling obstacles. Herein, we explore how recent advancements in sustainable chemistry emerge through DES enhanced with ML technology, while concentrating on solvent development and performance enhancement along with their broader impact on green chemistry fields.

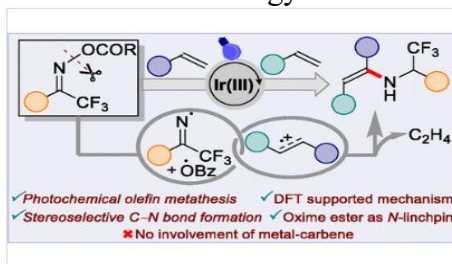


[Merging photochemical olefin metathesis with an amination reaction](#)

B Paul, S Das, SK Mahapatra, L Roy, I Chatterjee - ACS Catalysis, 2025

Abstract: A merger of photochemical olefin metathesis and C–H amination enables us to unlock a rare protocol for the synthesis of functionalized olefins. Our method allows for the stereoselective generation of enamines using a mild and bench-stable oxime ester precursor as the *N*-linchpin. The

key feature is the multitasking catalysis of *fac*-Ir(ppy)₃, which not only enables the energy transfer (EnT) mediated N–O bond cleavage of an oxime ester to produce an N-centered radical (NCR) and a benzoyloxy radical ([•]OBz) but also promotes the cycloaddition of two styrene moieties to form a cyclobutane analogue at different stages of the reaction. Further, mechanistic investigations and DFT calculations provide crucial insights on a rare ring-opening metathesis, prompted by the oxidation of the cyclobutane intermediate, followed by nucleophilic attack of an *in situ* generated benzoate anion ([−]OBz) and radical-coupling with NCR leading to a highly stable singlet intermediate that undergoes sequential *N*-protonation and single electron reduction to effectuate elimination and regeneration of [•]OBz, delivering the *Z*-selective aminated stilbene. Reasonable functionality tolerance, in addition to satisfactory yield and exclusive stereoselectivity are the salient features of this newly discovered methodology.



[Mixed addenda polyoxometalates by cooperative self-assembly and modulation of their optoelectronic properties](#)

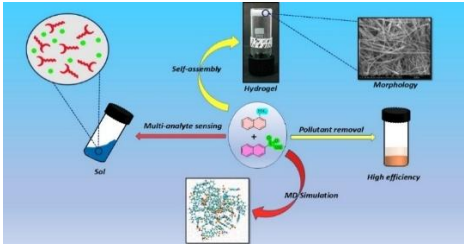
G Singh, R Choudhary, D Mandal - *Inorganic Chemistry Frontiers*, 2025

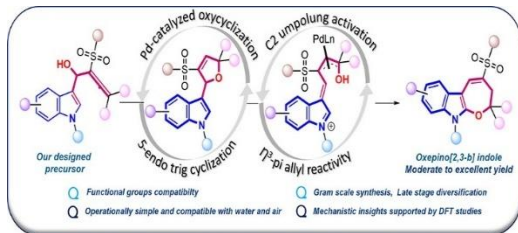
Abstract: Orbital engineering through the cooperative effect of different transition metals (TMs) is a powerful and versatile approach for modulating the chemistry of polyoxometalates (POMs), either by introducing novel POM structures or by designing POM hybrids for more effective catalytic applications. Here, we present a cooperative mixed-metal strategy for the synthesis of mixed-addenda (Mo/W) sandwich POMs with varying compositions, denoted by the general formula [(TM_i)₂(TM_e)₂(H₂O)₂(XMo_xW_{9-x}O₃₄)₂]^{n−} (TM_e(2+) = Fe/Co/Ni/Zn and TM_i(3+) = Mn/Fe, X = Zn/Co/Fe). Using this cooperative mix-metal strategy, overall, we report 24 new POMs, including 8 mixed-addenda, 12 W-based sandwich POMs, and 4 POM-based 1-D coordination frameworks. Structural analyses reveal that Mo-addenda incorporation into the POM framework, alongside W (Mo/W), is strongly influenced by the variation of the transition metal composition at the sandwich core, their oxidation states, and the pH of the reaction media. Electrospray ionization mass spectrometry (ESI-MS) and energy dispersive X-ray (EDAX) analysis confirm the detailed POM compositions, while UV-vis spectroscopy and complementary density functional theory (DFT) analysis provide insights into orbital engineering *via* distinctive charge transfer processes. Theoretical and electrochemical studies demonstrate that electron transfer modulation occurs through both mixed-addenda incorporation and mixed-metal substitution at the sandwich position. This is further elucidated by enhanced oxygen evolution (OER) activity, where the cooperative mixed-metal and mixed-addenda POMs exhibit significantly improved performance, with an overpotential of 500 mV at 1 mA cm^{−2}, compared to 570 mV in a pH 7.1 buffer. Additionally, this cooperative mixed-metal, mixed-addenda strategy extends to the formation of 1-D polyoxometalate coordination frameworks (POMCFs), where the oxidation state of precursor metals plays a vital role in determining the overall structural attributes.

54.	<p>MoSe₂@ MoO₂ hybrid nanostructures decorated with gallium nanoparticles for room temperature hydrogen gas sensor R Rovins, S Kumar, A Kumar, G Bassi, M Kumar, M Kumar - Nanotechnology, 2025</p> <p>Abstract: Hydrogen (H₂), a clean and sustainable energy carrier, is crucial in global efforts toward decarbonization and environmental sustainability. However, its flammability and explosiveness at concentrations exceeding 4% necessitate precise, real-time monitoring to ensure safety in industrial and domestic applications. Conventional H₂ gas sensing technologies have several limitations, such as high cost, complexity, cross-sensitivity, sensor drift, and elevated operating temperatures. To address these challenges, we fabricated a highly sensitive and selective H₂ sensor using Gallium nanoparticles (Ga NPs) decorated MoSe₂@MoO₂ hybrid nanostructures working at room temperature (RT). The hybrid of MoSe₂@MoO₂ was grown using the chemical vapor deposition (CVD) technique, and further, the grown film was decorated with Ga NPs to enhance its sensing performance. The hybrid nanostructures exhibited an ~11% response to H₂ at 30 °C, with notable issues in recovery and selectivity. By incorporating Ga NPs with an optimized concentration of 10 μl, the sensor achieved an enhanced response of ~47% at 30 °C (i.e.4.3 times increase in sensor response) with tremendous selectivity towards NO₂, CO₂, H₂S, and NH₃ gases, and the sensor shows a lower limit of detection (LOD) of 47.8 ppb. The sensor demonstrates a fast response and recovery time, exceptional durability, and prolonged stability. This improvement is attributed to the synergistic interaction between the hybrid nanostructures and the catalytic properties of Ga NPs, enabling superior response, stability, and selectivity at RT. This work illustrates a considerable improvement in semiconductor-based hydrogen sensing by proposing a robust, cost-effective, and energy-efficient solution. The proposed sensor demonstrates strong potential for next-generation gas sensing technologies, providing a portable and reliable platform for real-time hydrogen monitoring in various applications.</p>
55.	<p>Multi-opinion based method for quantifying polarization on social networks M Singh, SRS Iyengar, R Kaur - Journal of Computational Social Science, 2025</p> <p>Abstract: Social media platforms have emerged as a hub for political and social interactions, and analyzing the polarization of opinions has been gaining attention. In this study, we have proposed a measure to quantify polarization on social networks. The proposed metric, unlike state-of-the-art methods, does not assume a two-opinion case and applies to multiple opinions. We tested our metric on different networks with a multi-opinion scenario and varying degrees of polarization. The scores obtained from the proposed metric were comparable to state-of-the-art methods on binary opinion-based benchmark networks. The technique also differentiated among networks with different levels of polarization in a multi-opinion scenario. We also quantified polarization in a retweet network obtained from Twitter regarding the usage of drugs like hydroxychloroquine or chloroquine in treating COVID-19. Our metric indicated a high level of polarized opinions among the users. These findings suggest uncertainty among users in the benefits of using hydroxychloroquine and chloroquine drugs to treat COVID-19 patients.</p>

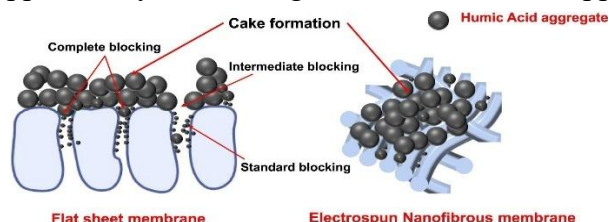
56.	<p>Ohmic contact to Schottky conversion on mitigating the oxygen defects present at the Ni/MgO-Ga₂O₃ interface Shivani, S Dahiya, RB Marathe, AG Chakkar, P Kumar, M Kumar - Journal of Physics D: Applied Physics, 2025</p> <p>Abstract: Gallium oxide (Ga₂O₃) holds significant potential for next-generation power devices with its intrinsic capability to hold a higher electric field than conventional semiconductors before its breakdown. However, the operation of Ga₂O₃-based power devices and their figure-of-merit are significantly influenced by the quality of metal–Ga₂O₃ contacts and interface defects. Here, we report the influence of oxygen vacancies on the electronic properties of Ni/MgO–Ga₂O₃ metal–oxide–semiconductor interfaces. We explore the interface between Ga₂O₃ and a thin MgO layer with variable oxygen vacancies for Schottky barrier diodes (SBDs). A Ni/MgO–Ga₂O₃ stack with 0% oxygen flow during MgO growth offers a rather leaky (ohmic) characteristic owing to the existence of oxygen defects at the Ni/MgO–Ga₂O₃ interface. However, for MgO film with 66% oxygen flow during its growth, the Ni/MgO–Ga₂O₃ SBD exhibits a rectifying behaviour as a result of the compensated oxygen vacancies. X-ray photoelectron spectroscopy and frequency-dependent capacitance–voltage and conductance–voltage characteristics were analysed to elucidate the mechanisms of the transition from ohmic to Schottky behaviour of the contact. This study paves the way for understanding and controlling interface defects, which are essential for advancing the development of next-generation power electronics.</p>
57.	<p>On the natural attenuation of leaching hexavalent chromium by ambient-soil and associated health-risks: characterization and adsorption studies S Ganguly, S Ganguly - Results in Engineering, 2025</p> <p>Abstract: Hexavalent chromium [Cr(VI)] contamination in the subsurface presents a significant challenge to environmental sustainability and public health. Its mobility and dispersion are highly dependent on soil properties, which can either promote natural attenuation through adsorption by the soil particles, or create pathways that facilitate its transport, increasing the risk of groundwater pollution. This study evaluates the natural ambient soil’s potential to adsorb Cr(VI) and identifies key influencing factors such as dose, pH, contact time, and initial Cr(VI) concentration to optimize adsorption efficiency. To obtain deeper insights, Electrical Resistivity Tomography (ERT) is utilized to evaluate the lithological features of the study area, complemented by advanced characterization techniques to analyse the soil’s microstructural characteristics and chemical constituents. Adsorption isotherm and kinetic studies were conducted to elucidate the adsorption mechanism and identify the rate-limiting steps, respectively. Furthermore, the study quantifies potential risks to human health, including carcinogenic and non–carcinogenic effects associated with residual Cr(VI) concentrations in contaminated water, underscoring the critical need for effective remediation strategies and the restoration of public health safety. The study findings revealed a residual Cr(VI) concentration of 0.583 mg/L—significantly exceeding the World Health Organization’s (WHO’s) permissible limit of 0.05 mg/L. This alarming level underscores the critical need for health–risk assessments, which indicated a “very high” total cancer risk and “very high” non–cancer risks for both the male and female populations.</p>
58.	<p>On the units in group rings over Z_n H Setia, S Kaur, M Khan - Periodica Mathematica Hungarica, 2025</p> <p>Abstract: Let n be an integer co-prime to 3 and let Z_n be the ring of integers modulo n. In this article, we study the structure and generators of the unit group of $Z_n C_3$. Further, if T_m denotes the elementary abelian 3-group of order 3^m, then we provide the structure of $U(Z_n T_m)$. We also solve the normal complement problem in each case.</p>

59.	<p>Plasticity-based approaches for infinite slope analysis of nonlinear bonded soils R Ganesh - International Journal of Geomechanics, 2025</p> <p>Abstract: The instability potential of slopes prone to shallow sliding is commonly analyzed using the infinite slope model, with most existing research based on the linear Mohr–Coulomb failure criterion. However, many bonded geomaterials generally exhibit nonlinear yield behavior. This paper presents a novel semianalytical solution procedure to investigate the potential for infinite slope collapse in bonded soils characterized by a general nonlinear power-law type failure criterion. The upper and lower bound theorems of plasticity were applied to conduct the present investigations, with results expressed in terms of the stability factor and factor of safety. The mechanical effects of groundwater flow on the failure potential of slopes were also considered through a modified pore pressure parameter under varying flow conditions. Numerical results indicate that the upper and lower bound solutions are identical, confirming that the obtained solution is exact. The results are presented in the form of charts, which are useful for assessing slope safety and understanding the mechanical effects of different parameters that characterize the behavior of nonlinear bonded soils.</p>
60.	<p>Reliability assessment using electrical and mechanical characterization of stretchable interconnects on ultrathin elastomer for emerging flexible electronics system G Bhatti...R Sharma, MG Kumar - IEEE Transactions on Components, Packaging and Manufacturing Technology, 2025</p> <p>Abstract: Stretchable electronics is one of the emerging technologies that empowers electronic circuits to gracefully adjust to their surroundings by elongating when subjected to external forces. Integrating stretchable interconnects with deformable materials and optimum geometries establish a path to high-performance stretchable electronics. The amount of stretch and bend that stretchable interconnect can endure while maintaining functionality are the critical important parameters. This paper aims to illustrate the mechanical impact of the elastomeric substrate on the stretchable interconnect. In the present analysis, polydimethylsiloxane (PDMS) elastomeric substrate is considered. Five different stretchable interconnect structures viz. straight (St), zigzag (Zz), serpentine (Sp), horseshoe (Hs) and rectangle (Rt) are considered. The electrical parameters, viz. resistance (R), inductance (L) and capacitance (C) are extracted for all the considered stretchable interconnects to assess the conductivity of the interconnect under deformation effects. Further, the Manson formulation based strain life cycle is formulated and fatigue cycle test is performed using finite element analysis (FEA) based method on ANSYS workbench, which confirms the mechanical reliability of the considered stretchable interconnects. The signal integrity analysis of the considered interconnects is performed at varying frequencies. Finally, the interconnect models are verified using experimental model results.</p>
61.	<p>Supramolecular gels from sulfonic acid-containing two-component gelators: Molecular dynamics simulation, dye absorption and multianalyte sensing studies AT Meitei, M Moirangthem, N Yaiphaba, SK Meena, RS Singh - Langmuir, 2025</p> <p>Abstract: We investigated the design and gelation behavior of some two-component supramolecular gels formed from two sulfonic acids, <i>i.e.</i>, naphthalene-2-sulfonic acid and (1<i>R</i>)-(–)-10-camphorsulfonic acid paired with various organic amines. This study utilized experimental characterizations, functional studies and molecular dynamics (MD) simulations to study the gelation process. Remarkably, many of these two-component gelators successfully gelled multiple organic solvents and water, while the sulfonic acids or the amines did not individually. This underscores the critical synergistic role that both components play in gel formation. We conducted</p>

	<p>comprehensive FTIR, XRD, SEM, and rheological characterizations of the hydrogel and some organogels. MD simulations were also performed to evaluate the gels' RDF, CN, H-bonding, and partial density and explore gelation dynamics. A good correlation was observed between the predicted aggregation behavior from both experimental characterization and MD simulation. The findings confirm that gel formation is driven by secondary interactions, including H-bonding, ionic interactions, π-π stacking, and solvophobic forces, which promote gelator aggregation and supramolecular organization. Remarkably, naphthalene-2-sulfonic acid and 1-naphthylamine formed hydrogels across an extensive pH range of 0.2 to 12, which is uncommon among other gelators. The morphologies of these hydrogels exhibited pH dependence, indicating the presence of varying aggregation mechanisms. Furthermore, we have demonstrated several applications for this hydrogel. It effectively removed two water-soluble dyes, methylene blue and crystal violet, from their aqueous solutions. Moreover, the hydrogel can detect a variety of analytes. Upon exposure to volatile organic amine vapors, hydrogel films rapidly melt, providing a straightforward method for detecting amines without the necessity for sophisticated instruments. Trifluoroacetic acid and methanol were also detected similarly, albeit with longer response times. Overall, this work highlights the efficient preparation of multifunctional two-component gels using simple and commercially available sulfonic acids, thus eliminating the need for the tedious and time-consuming synthesis of gelators.</p> 
62.	<p>Tensor tomography for a set of generalized V-line transforms in \mathbb{R}^2 R Bhardwaj - Analysis and Mathematical Physics, 2025</p> <p>Abstract: We study a set of generalized V-line transforms, namely longitudinal, mixed, and transverse V-line transforms, of a symmetric m-tensor field in \mathbb{R}^2. The goal of this article is to recover a symmetric m-tensor field $\{f\}$ supported in a disk D_R, with radius R and centered at the origin, by a combination of the aforementioned generalized V-line transforms, using two different techniques for different sets of data.</p>
63.	<p>Understanding the early stage (< 10 min) oxidation behaviour of a multi-principal element cobalt base solid solution superalloy at 1000° C V Polimetla, A Anupam, N Koundinya, ASM Ang, CC Berndt, RS Kottada - Corrosion Science, 2025</p>

	<p>Abstract: The formation of transient oxides (spinel and/or mixed) with a higher growth rate during the early-stage (< 10 min) of high-temperature oxidation, inevitably influences the evolution of steady-state protective oxide. A new approach of using the faster heating mode of the Gleeble thermomechanical simulator to study the early-stage oxidation of high-temperature alloys at 1000 °C has been proposed. Unique and advantageous features of Gleeble, such as higher heating and cooling rate and, a controlled atmosphere, make this method suitable to investigate the oxide characteristics in the early-stage regime of oxidation exclusively. The method was demonstrated with the study on early-stage oxidation of solid solution strengthened multi-principal element Co-based superalloy at 1000 °C for 0, 100, 250 and 500 s. The detailed analysis of the chemical evolution and composition of the oxide scale within the studied regime is reviewed and discussed in detail.</p>
64.	<p>Unveiling palladium catalysis to access oxepino-indole through sequential oxycyclization utilizing η^3-π-allyl reactivity P Singh, MV Mane, SK Mahto, AC Shaikh - Organic Letters, 2025</p> <p>Abstract: We report a palladium-catalyzed sequential oxycyclization of indole-tethered allene to construct oxepino indole cores with yields up to 91%. This method showcases the C2 umpolung activation of indoles via η^3-π-allyl reactivity and enables efficient synthesis without side products. Furthermore, extensive mechanistic investigations, encompassing control experiments, X-ray crystallographic studies, and DFT analysis, have been conducted to elucidate the underlying mechanisms. Additionally, gram-scale synthesis and product diversification have been performed to illustrate the synthetic utility of this transformation.</p>  <p>Our designed precursor</p> <p>Pd-catalyzed oxycyclization</p> <p>C2 umpolung activation</p> <p>Oxepino[2,3-b]indole</p> <p>Moderate to excellent yield</p> <p>Functional groups compatibility</p> <p>Operationally simple and compatible with water and air</p> <p>Gram scale synthesis, Late stage diversification</p> <p>Mechanistic insights supported by DFT studies</p>
65.	<p>Unveiling the mechanisms of organic matter fouling and transport properties in silver nanowire-infused core-shell nanofibrous membranes V Sharma, PR Junghare, Nazreen V. M, SP Gumfekar - Separation and Purification Technology, 2025</p> <p>Abstract: Organic matter from groundwater and industrial effluents severely impact the performance and lifespan of membranes by fouling. The pH and ionic strength of organic matter containing feed solutions further influence membrane fouling by altering solubility. The close relationship between membrane transport properties and fouling ultimately determines filtration efficiency. In this work, we analyzed fouling of Electrospun Nanofibrous Membranes (ENM) exposed to Humic Acid (HA). ENM composed of polysulfone nanofiber shell and silver nanowires (AgNW) core. Effect of pH on fouling ratios, rejection efficiencies, and fouling coefficients represented the fouling propensity of ENM. AgNW-containing membranes revealed higher flux decline due to HA fouling. Acidic pH induced extensive HA aggregation, exacerbating flux decline, particularly in membranes with AgNW incorporation. However, AgNW-enhanced membranes exhibited antifouling properties under acidic conditions, achieving 68.4% flux recovery. AgNW incorporation significantly improved HA rejection, increasing rejection rates from 19.2% to 57.8% at alkaline pH. Further, we fitted single and combined fouling models to the</p>

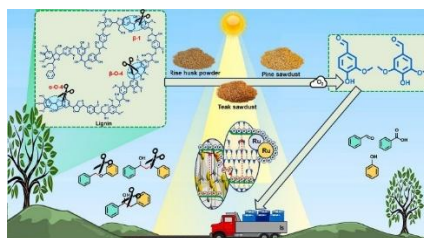
experimental data to identify the dominating fouling mechanism. Cake formation emerged as the primary fouling mechanism, with the cake filtration coefficient increasing as AgNW concentration rose. Combined fouling model showed negligible pore-blocking effect. Furthermore, AgNW containing ENM showed less rate of flux decline under high-ionic strength foulant and industrial feed. Hence, this study provides a fundamental understanding of fouling and transport mechanisms while offering practical applicability for real organic matter removal applications.



[Visible-light photocatalytic depolymerization of waste-derived lignin into renewable aromatics, vanillin and syringaldehyde, over Ru@OCN/FeVO₄](#)

R Ghalta, R Srivastava - Journal of Catalysis, 2025

Abstract: Lignin valorization remains a grand challenge due to its structural complexity and the resistance of key interunit linkages β -O-4, α -O-4, and β -1 to cleavage under mild conditions. Herein, we unveil a Ru-decorated Z-scheme photocatalyst (Ru@OCN/FeVO₄) that drives selective and efficient oxidative lignin depolymerization under mild conditions using molecular oxygen. The catalyst integrates oxygen-doped carbon nitride (OCN) with FeVO₄ to construct a Z-scheme heterojunction, which enhances visible-light absorption, charge separation, and reactive oxygen species (ROS) generation. The incorporation of Ru nanoparticles further facilitates electron trapping and molecular oxygen activation, driving the selective bond cleavage. The optimized catalyst achieves remarkable conversions of lignin model compounds, with β -O-4 (98.7%), α -O-4 (91.2%), and β -1 (98.2%) linkages, yielding aromatic monomers such as benzaldehyde and phenol with high selectivity. Furthermore, it effectively processes native lignin from diverse sources (hardwood, softwood, rice husk), achieving depolymerization yields of up to 71% and demonstrating feedstock-dependent monomer selectivity, notably syringaldehyde (55%) from hardwood and vanillin (74%) from softwood. Comprehensive structural and product analyses using HSQC NMR, GPC, and GC-MS establish a strong correlation between lignin architecture, bond cleavage efficiency, and monomer distribution. In-depth mechanistic studies, including in-situ XPS, UPS, EPR, isotope-labelling, and DMPO-radical trapping, reveal that the reaction proceeds via a direct Z-scheme charge transfer and ROS-mediated β -C-H abstraction pathway. This work offers a sustainable and scalable strategy for lignin valorization, effectively coupling advanced photocatalysis with real-world biomass conversion, and showcases the potential for industrial implementation within the circular bioeconomy.



Disclaimer: This publication digest may not contain all the papers published. Library has compiled the publication data as per the alerts received from Scopus and Google Scholar for the affiliation “Indian Institute of Technology Ropar” for the month of July, 2025. The author(s) are requested to share their missing paper(s) details if any, for the inclusion in the next publication digest.